AJNR Am J Neuroradiol 19:261–266, February 1998

The Cerebral Effects of Carbon Dioxide during Digital Subtraction Angiography in the Aortic Arch and Its Branches in Rabbits

Panos B. Dimakakos, Theodoros Stefanopoulos, Anthony G. Doufas, Maria Papasava, Athanasios Gouliamos, Demetrios Mourikis, and Helene Deligiorgi

***PURPOSE*: We studied the neurotoxicity of carbon dioxide as a contrast agent in the central nervous system by performing CO_2 digital subtraction angiography (DSA) in the aortic arch and its branches in experimental animals.**

***METHODS*: Twenty-five rabbits underwent intraarterial CO_2 DSA while under general anesthesia, during which 50 angiograms were obtained after administration of 3 mL/kg CO_2. MR imaging was performed before and after the angiographic procedure. The animals were killed 12 hours later and their brains examined macroscopically and microscopically.**

***RESULTS*: Three animals died of a cause irrelevant to CO_2. No animal had clinical symptoms of hemiplegia or stroke. Neither MR imaging nor macroscopic and microscopic examination of the brain revealed any ischemic infarct hemorrhage, thrombosis, or foci of necrosis.**

***CONCLUSION*: The absence of neurologic symptoms, the lack of pathologic findings at MR imaging, and the negative pathologic findings in the brain encourage further research on CO_2 neurotoxicity of the central nervous system and support its application in the imaging of intracranial vessels.**

The use of carbon dioxide as a contrast medium allows the same characterization of radiologic images as do iodinated contrast agents but avoid the possibility of an allergic reaction or renal failure, the frequency of which reaches as high as 20% (1–4). Most experimental and clinical studies have shown that intravenous and intraarterial administration of CO_2 is safe (3–12), except for neurotoxic reactions in the central nervous system (CNS) of mice, caused by damage to the endothelial cell membrane resulting in multifocal ischemic infarcts and neurologic deficits (13). On the other hand, another study with CO_2 administration in the thoracic aorta and the carotid arteries in dogs did not produce any neurologic deficits or electroencephalographic or gross pathologic changes (14).

The present study investigated toxicity in the CNS in rabbits after administration of CO_2 in conjunction with digital subtraction angiography (DSA) in the aortic arch or, selectively, in the carotid and vertebral arteries.

Received March 14, 1997; accepted after revision July 2.

From the Departments of Vascular Surgery (P.B.D., M.P.), Hemodynamics and Angiography (T.S., D.M.), Anesthesiology (A.G.D.), MRI and Computed Tomography (A.G.), and Pathology (H.D.), Aretaieion Hospital, University of Athens (Greece).

Address reprint requests to Panos B. Dimakakos, MD, 27-29 Alopekis St, 106 75 Athens, Greece.

Methods

Twenty rabbits with a mean weight of 2.7 kg were used for this experimental study. An additional five rabbits were used as comparative controls.

The animals were premedicated with 0.5 mg/kg midazolam (Dormicum, Roche, Switzerland) and 0.04 mg/kg fentanyl (Janssen Pharmaceutica, Belgium) intramuscularly. After a marginal ear vein was cannulated, they were anesthetized by intravenous administration of 30 to 40 mg/kg thiopental sodium (Pentothal, Abbott, Italy) as an initial dose, and anesthesia was maintained with supplemental administration of 10% of the above thiopental dose every hour. Cricothyroidotomy was performed, through which an endotracheal uncuffed tube (3-mm internal diameter) was placed into the trachea. Ventilation was controlled manually after the animals were paralyzed with 0.2 mg/kg pancuronium bromide (Pavulon, Organon Teknika, Belgium), followed by additional doses as required. We used a Mapleson C (Mia United Kingdom) rebreathing system in which both fresh gas flow (oxygen in nitrogen; fractional inspired O_2, 0.4 and ventilation 2L/min) were 50% greater than resting minute volume in order to achieve normocapnic conditions ($Paco_2$ 35 to 45 mm Hg; pH_a, 7.35 to 7.45) (15). A polyethylene catheter (20-gauge) was inserted into an artery for arterial blood gas sampling and hemodynamic measurements. A pulse oximeter with an ear probe was used for arterial oxygen saturation (SaO_2) and pulse rate monitoring. Ringer's lactate solution was infused at a rate of 4 to 10 mL/kg per hour throughout the experiment.

We applied near-infrared spectroscopy (Criticon Cerebral RedOx Monitor Model 2020) to determine cerebral oxygenation and hemodynamics in the animals throughout the experiment. Near-infrared spectroscopy provides continuous real-time quantified values for the concentration of oxyhemoglobin (HbO_2), deoxyhemoglobin (HHb), and total hemoglobin (tHb) in the tissue. The signal for cytochrome oxidase is not fully quantified, but shows quantified changes in the concentration of the above chromophore (16, 17). Regional oxygen saturation (rSO_2) is the percentage of HbO_2 in relation to the total hemoglobin (rSO_2 = HbO_2* 100/HbO_2 + HHb) and is automatically calculated by the above monitor. It should be noted that the cerebral tissue under spectroscopy contains not only arterial but also venous blood, thus rSO_2 is a mixed arteriovenous measurement and the value will be lower than that obtained by using a pulse oximeter (SaO_2), which estimates only the saturation of the pulsatile (arterial) component of blood flow. Changes in the cerebral blood volume (CBV), which reflect changes in the perfusion state of the brain (18–21), were easily inferred from changes in the tHb concentration.

Before and immediately after each CO_2 injection into the aorta, or selectively into the internal carotid artery, blood samples were drawn from the catheterized artery to check pH, PaO_2, and $PaCO_2$, and the animal's blood pressure was monitored invasively.

Following completion of the above procedure, the femoral artery was sectioned and paracentesis of the radial artery was performed with an arrow-type 22-gauge catheter. A hydrophilic 25-inch, 64-mm guidewire (Meadox) was then propelled as far as the aortic arch under fluoroscopic guidance followed by introduction of a pediatric 3F head catheter into the aortic arch or, selectively, into the common carotid or vertebral artery. Periodic administration of 1 to 2 mL of heparinized serum was used to avoid clotting the catheter; also 1 mL of blood was taken to check blood gases. The catheter was subsequently filled with heparinized serum and connected to the system delivering the CO_2.

Five control animals were initially used to establish and compare normal parameters of magnetic resonance (MR) imaging and angiography of the aortic arch and its branches performed with typical, iodinated contrast material.

Before infusion, the syringe was coupled to a continuous CO_2 flow and the plunger was placed beneath the CO_2 flow. The plunger was then joined to a catheter system, which, after each connection with the continuous CO_2 flow, was immersed into heparinized serum and drawn as far as the syringe. The continuous flow of CO_2 and the closed circuit of catheter-syringe full of serum prevented the introduction of air bubbles. Each injection included 3 mL/kg of pure CO_2 injected via a disposable inflation device (Wizard II, USCI), which guaranteed exact control of quantity and approximate control of pressure applied. With the animal in an apneic state, angiograms were obtained at a rate of three per second during a period of 4 seconds. The CO_2 was administered with intervals of at least 3 minutes between each dose, while the animal's head was slightly elevated to 45° to avoid the pooling of bubbles into the arterial system. Angiograms were reviewed by two radiologists, who rated diagnostic accuracy and image quality subjectively on a scale of 1 to 4 as compared with the control animals (1 = excellent, 2 = very good, 3 = good, 4 = bad). MR imaging before and 8 hours after the experiment included axial T_1-weighted spin-echo images (450/25/4 [repetition time/echo time/excitations]), coronal T2-weighted images (2000/100/2), and proton density–weighted images (200/25/2) with 5-mm-thick sections, a 25-cm field of view, and a 192 × 192 matrix.

The animals were killed 12 hours later, and the brains of all 25 rabbits were removed, fixed in 10% buffered formalin for 48 hours, and serially cut into 0.5-cm-thick coronal sections. Twenty-four tissue blocks were sampled from each brain, 20 from the cerebrum, three from the cerebellum, and one from the medulla. The 1 × 1 × 0.5-cm tissue blocks were embedded in paraffin, cut at 4 μm, and stained with hematoxylin-eosin.

Results

A total of 50 angiographic procedures were carried out, and an average of 29.15 mL of CO_2 was given to each experimental animal (Table 1). Thirty-two images of the aortic arch, 14 of the carotid arteries, and four of the vertebral arteries were taken selectively.

During the injection of CO_2, no significant changes in arterial blood gases or SaO_2 were observed under any volume and pressure conditions we used, whereas the mean arterial pressure increased about 15 to 25 mm Hg soon after the injection and decreased to the preinjection level 1 to 2 minutes later. The pulse rate, indirectly detected from the pulse oximeter, showed a remarkable decrease during and immediately after the CO_2 injection. Soon after that, a rise in pulse rate to a higher than preinjection level was observed. Paralysis of the animals prevented us from observing any change in respiratory rate that might have been caused by CO_2 injection. However, in a few animals, which during the initial setup of the experiment had not been paralyzed, the intracarotid CO_2 injection led at first to slow and deep breaths and later to irregular respiration with random deep and shallow breaths. The near-infrared spectroscopy monitor showed a reduction in tHb at the time of injection, and a simultaneous reduction in rSO_2. On the other hand, the immediate postinjection phase was characterized by a marked increase in tHb even beyond the preinjection levels, while rSO_2 remained low. Unfortunately, our cytochrome oxidase measurements were insufficient and not of good quality because of a high interference index in the cytochrome oxidase trace. During the period following anesthesia, no signs of hemiplegia or stroke were observed.

DSA afforded good visibility of the aortic arch and its tributaries (Fig 1). Both large and medium-sized arteries were also judged satisfactorily as compared with conventional angiography (Fig 2). At an atmospheric pressure of 1 to 1.5 atm, at which CO_2 was administered, imaging of the arterial system enabled concomitant visualization of the aortic arch and its branches as well as the inferior aorta (Fig 3). Imaging of the carotid and vertebral arteries was selectively determined (Fig 4). By consensus, the two interpreters rated all images as either grade 2 (very good) or grade 3 (good).

Three of the experimental animals died (numbers 2, 4, and 15), but these deaths seem to be unrelated to CO_2 administration.

Comparative preoperative and postoperative control MR imaging showed an absence of ischemic infarct or hemorrhage during a mean period of 10 hours after CO_2 DSA; brain edema only in animals 2 and 4; and, in two other animals (numbers 9 and 10), three to five round black spots approximately 2 mm in diameter, in symmetric sites of both hemispheres. These spots were present with homogeneous imaging of the brain matter, which we consider typical for imaging vessels or cerebrospinal fluid in the subarachnoid space.

Animals and angiographic techniques

Animal	Weight, kg	Angiographic Vessel	Quantity of Carbon Dioxide, mL	Pressure, atm	Observations
1	4.2	Aortic arch	15	1	Aortic arch and its branches
			10		
			10		
2*	4.3	Aortic arch	15	1	Continuous administration without free inverval;
			12	12	somnolence, spasm, death.
		Aortic arch and intracranial vessels	15		
			16		MR: cerebral edema
3	3.1	Aortic arch	20	1.5	Aortic arch, L carotid artery, and intracranial vessels
		L carotid artery	5		
4*	2.8	Aortic arch	15	1.5	Loss of blood, administration of fluids, cerebral
			15		edema (established through MR and histology)
		L vertebral artery	8		
			8		
5	2.7	Aortic arch	16	1	Aortic arch, R carotid artery, and intracranial vessels
		R carotid artery	10		
			8		
6	2.4	Aortic arch	15	1.5	Aortic arch and its branches
			12		
			12		
7	3.0	L carotid artery	9	1	Selective imaging of L carotid artery and branches of aortic arch
		Aortic arch	9		
			10		
8	3.1	Aortic arch	10	1	Aortic arch and its branches
			10		
9	3.5	Vertebral artery	12	1	L vertebral artery and L carotid artery. MR: black spots
		L carotid artery	10		
10	3.0	L carotid artery	8		Angiography: L carotid artery and aortic arch with its branches. MR: black spots
		Aortic arch	10		
			10		
11	2.6	Aortic arch	8	1	Aortic arch and its branches
12	2.8	Aortic arch,	8		Aortic arch and its branches, selectively R
		R carotid artery	9		carotid and L vertebral artery
		L vertebral atery	9	1	
13	2.5	Aortic arch	8	1	Aortic arch and R carotid artery
			8	1.5	
		R carotid artery	8	1	
14	2.5	R carotid artery	8	0.5	Selective imaging of R carotid artery
			8		
15*	2.3	Aortic arch	8	1	Respiratory disturbances
			10		
16	2.3	Aortic arch	8	1	Aortic arch and its branches
17	2.5	Aortic arch	8	1	Aortic arch and selective R carotid artery
		R carotid artery	8		
18	2.3	Aortic arch	8	1	Aortic arch and its branches
19	2.6	Aortic arch	8	1	Aortic arch and selective L carotid artery
		L carotid artery	8		
20	3.0	Aortic arch	9	1	Aortic arch with its branches and selective R carotid artery
			9		
		R carotid artery	10		

* These animals died, but the deaths seemed unrelated to CO_2 administration.

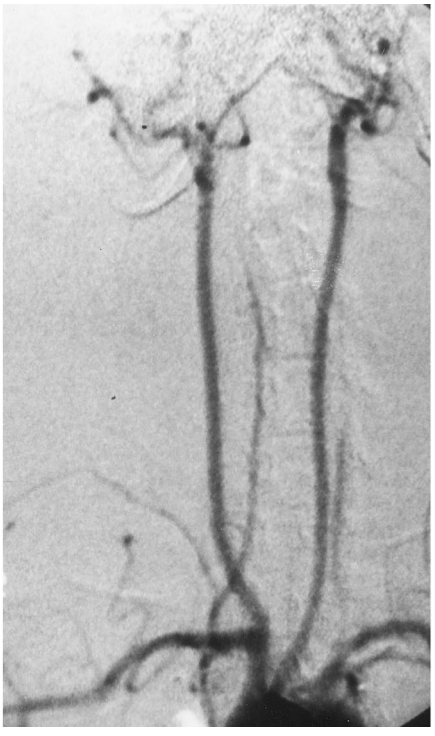

FIG 1. Angiogram of aortic arch and its branches after intraarterial infusion of CO_2 via placement of catheter tip in the ascending aorta.

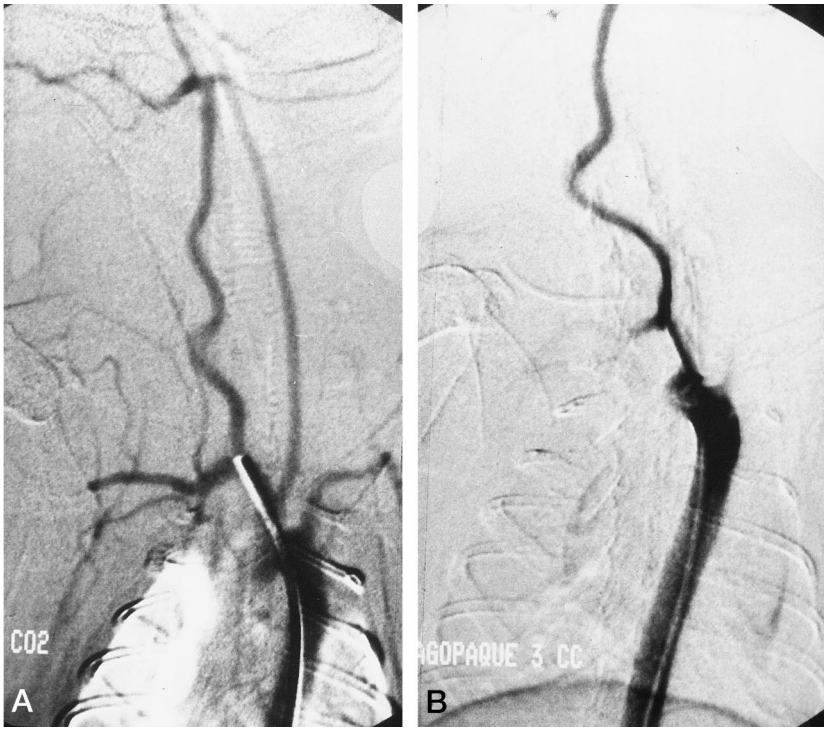

FIG 2. Comparative selective images of right vertebral artery with 8 mL CO_2 (*A*) and with 3 mL of typical contrast material (Imagopaque) (*B*) after insertion of the tip of the catheter into the orifice of the right common carotid artery.

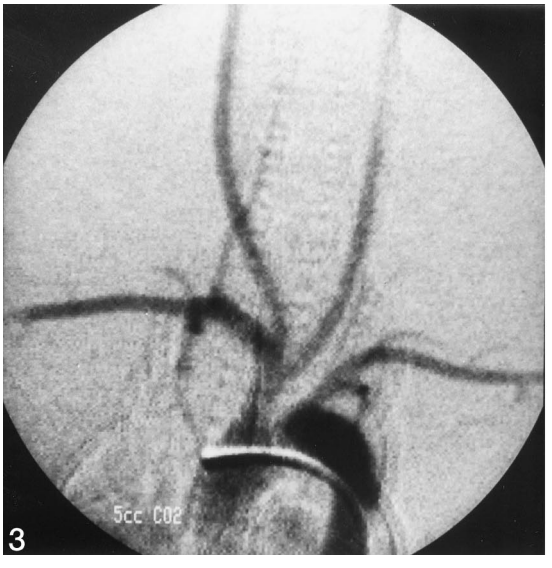

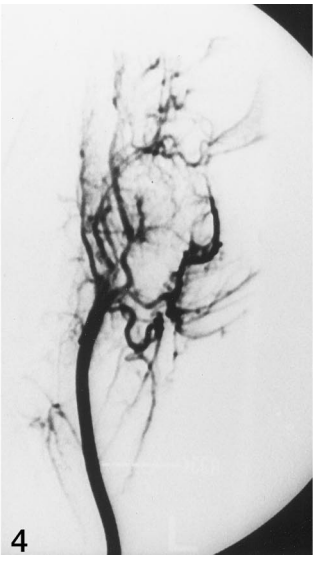

FIG 3. Angiogram of the aortic arch and its main branches together with the lower thoracic aorta after insertion of the tip of the catheter into the ascending aorta.

FIG 4. Selective image of the right common carotid artery after administration of 3 mL CO_2.

Gross examination of the 25 brains showed only slight congestion of the meninges. There was no evidence of any other changes. The vessels were unremarkable, the ventricles contained clear fluid, and there were no foci of necrosis in the brain substance. Microscopic examination showed moderate extracellular edema in the two rabbits (numbers 2 and 4) that died. There was no evidence of thrombosis, hemmorrhage, or ischemic necrosis in any of the other rabbits. The brains of the control animals were unremarkable.

Discussion

Carbon dioxide was used as a radiologic contrast medium in humans 40 years ago, but it is difficult to administer and the subtle difference in density between the contrast medium in the blood vessels and the surrounding soft tissues requires the use of DSA (22, 23).

In 1982, Hawkins (24) used CO_2 DSA to visualize the splanchnic arteries and arteries in the lower extremities in 20 patients. One year later, Miller et

al (9) used the same procedure to visualize the abdominal aorta and more distal arteries in nine patients without complications.

Although CO_2 may be characterized as a contrast agent of choice, especially in patients with renal insufficiency or a history of allergy, it has not managed to displace iodinated contrast agents, despite its low cost. The reason pertains to the lack of a reliable, safe, and easy method of administration, as well as to certain undesirable characteristics of CO_2 (invisibility, susceptibility to air contamination, pooling of gas bubbles) and the possibility of neurotoxicity. The administration of CO_2 in the carotid arteries of mice has produced immediate dramatic neurologic deficits, disruption of the blood-brain barrier and of the endothelial cell membranes, and multifocal ischemic infarctions caused by the hypoxic effect of gas emboli, so that CO_2 might not be tolerated by the CNS of every mammal (13). Other investigators, on the basis of indirect measurements of the cerebral flow and brain electrical activity as end-points, have suggested that ischemia caused by small gas emboli is reversible (22, 23).

These ambiguous findings are probably due to technical weaknesses and to inconsistencies in the experimental models, including the mode of CO_2 administration (pressure, quantity, infusion time); the anatomic significance of the vessels in which the gas bubbles were trapped; and the kind and hemodynamic condition of the experimental animals used, which influence the time of lodging of the gas bubbles within the vessel (23). These data could explain the contradictory results obtained among different experimental specimens.

The dramatic and spiked effect of intracarotid CO_2 injection on pulse rate might well be related to a sharp increase in intracranial pressure and is a common clinical sign (similar to the respiratory disturbances in the nonparalyzed animals) in acute intracranial hemorrhage. The near-infrared spectroscopy monitor showed a reduction in rSO_2 at the time of injection, which, in combination with a negative change in CBV, indicated an acute diminution in cerebral blood flow (CBF) caused by the sudden increase in intracranial pressure (25), and resulted in extended HbO_2 desaturation (18).

On the other hand, the immediate postinjection phase was characterized by a marked increase in CBV, even beyond the preinjection levels, while rSO_2 remained low, a situation similar to the postischemic hyperemia observed even after an experimentally induced 30-second cessation of CBF (26, 27). This postocclusive overabundant CBF relative to metabolic needs is caused by a number of vasoactive metabolites generated during ischemia and by the early reperfusion period (28, 29). The direct local vasodilatation effect of the injected CO_2 and the slowing of the pulse rate caused by high intracranial pressure may also play a role in reversing the expected hemodynamic consequences described above (30, 31). In other experiments, in which systemic hypercapnia was induced either by breathing CO_2 (29) or by hypoventilating the subject (19), the CO_2-induced positive changes in CBF and CBV were associated with a decrease in the amount of HHb and a higher mean hemoglobin saturation (high rSO_2), which characterize a luxury-perfusion state. The reduced rSO_2 in the postinjection hyperemic phase in our experiment clearly indicates that there are different hemodynamics of a slower cerebral circulation (low CBF) arising from the acute increase in intracranial pressure lasting for some minutes after the intracarotid CO_2 injection, despite a simultaneous relative increase in mean arterial pressure. On the other hand, in cases of systemic hypercapnia, the less acute rise in intracranial pressure resulted in a faster circulation (high CBF) and a higher rSO_2.

Three experimental animals died: one (animal 2) had sustained a barotrauma, probably because of the excessive gas inflow during the manually controlled ventilation; the other one (animal 4) died of oligemic shock caused by extensive blood loss during the arterial catheterization procedure. The fluid administration, in combination with the low plasma colloid osmotic pressure and the subsequent brain damage due to protracted arterial hypotension (32, 33), might have resulted in global brain edema in this animal. In both animals, MR imaging showed edema that was confirmed by microscopic examination. The third death (animal 15), which occurred after a characteristic reaction (superficial breathing, slow pulse rate) observed immediately after infusion of CO_2, was probably due to a convergence of CO_2 at the coronary vessels or to a neurogenic syncope or strong parasympathicotonia caused by pressure from pneumonogastric nuclei.

In contrast to earlier studies of air embolization (31, 34) or intracarotid CO_2 injection (13), we found no clinically apparent neurologic deficits in any of the surviving animals. However, clinically evident neurologic dysfunction is not a prerequisite for the occurrence of the pathologic entity of multifocal microscopic infarcts (13, 35, 36).

According to Klatzo's classical work in the 1960s, brain edema may be classified into two major types, vasogenic and cytotoxic (37, 38). The original definition of *vasogenic edema* has remained essentially unchallenged, while cytotoxic edema has been reclassified into ischemic, osmotic, and interstitial edema (39). However, because both types of edema are frequently present, it is often impossible to classify a particular case as being one or the other (38, 40). The pathophysiology of cerebral edema in our animals was probably related to a mechanical or ischemic injury of the blood-brain barrier. Part of the pathologic changes in the structure of the blood-brain barrier were due to the action of numerous vasoactive metabolites generated in the ischemic period (during intracarotid CO_2 injection) and in the early reperfusion period (41–43). These postischemic excessive dilatory mechanisms in combination with the experimentally demonstrated marked increase in brain tissue osmolarity during the circulatory arrest period (29, 44) easily led to the production of a vasogenic

and simultaneously cytotoxic edema. The passage of the CO_2 bubble itself seems to be responsible for the endothelial membrane disruption; however, the precise mechanisms of membrane injury due to CO_2 embolization are not yet clearly understood (13). Physical deprivation of the liquid-phase contact or the shearing stress on the membrane as the gas-liquid meniscus passes, have also been implicated (13, 45).

Our experimental findings in rabbits, which included an absence of pathologic changes in anatomy or abnormal findings on MR images, as well as the good-quality images we obtained of the aortic arch and its branches, encourage further research on CO_2 neurotoxicity in the CNS and support its application in the imaging of intracranial vessels.

References

1. Cavo JJ, Trindade E, McGrecor M. **The risks of death and of severe nonfatal reactions with high-versus low-osmolarity contrast media: a meta-analysis.** *AJR Am J Roentgenol* 1991;156:825–832
2. Hess H. **Digitale Subtraktionsarteriographie mit Kohlendioxid: eine Alternative zur Extremitäten-arteriographie mit jodhaltigen kontrastmitteln.** *Fortschr Roentgenstr* 1990;153:233–238
3. Krasny R, Hollmann JP, Guenther RW. **Erste Erfahrungen mit CO_2 als gastroermiges Kontrastmittel in der DSA.** *Fortschr Roentgenstr* 1987;146:450–454
4. Kerns SR, Hawkins IF. **Carbon dioxide digital subtraction angiography: expanding applications and technical evolution.** *AJR Am J Roentgenol* 1995;164:735–741
5. Moore RM, Braselton CW. **Injections of air and carbon dioxide into a pulmonary vein.** *Ann Surg* 1940;112:212–218
6. Oppenheimer MJ, Durant TM, Stauffer HM, Steward GH, Lynch PR, Barrera I. **In vivo visualization of intracardiac structures with gaseous carbon dioxide: cardiovascular-respiratory affects and associated changes in blood chemistry.** *Am J Physiol* 1956;186:325–334
7. Durant TM, Stauffer HM, Oppenheimer MJ, Paul RE. **The safety of intravascular carbon dioxide and its use for roentgenologic visualization of intracardiac structures.** *Ann Intern Med* 1957;47:191–201
8. Sullivan KL, Bonn J, Shapiro MJ, Gardiner GA. **Venography with carbon dioxide as a contrast agent.** *Cardiovasc Intervent Radiol* 1995;18:141–145
9. Miller FJ, Mineau DE, Koheler PR, et al. **Clinical intraarterial digital subtraction imaging: use of small volumes of iodinated contrast material or carbon dioxide.** *Radiology* 1983;148:273–278
10. Weaver FA, Pentecost MJ, Yellin AE, Finck E, Teitelbaum G. **Clinical applications of carbon dioxide/digital subtraction arteriography.** *J Vasc Surg* 1991;13:266–273
11. Seeger JM, Self S, Harvard TRS, Flyn TC, Hawkins IF. **Carbon dioxide gas as an arterial contrast agent.** *Ann Surg* 1993;217:688–698
12. Kerns SR, Hawkins IF, Sabatelli FW. **Current status of carbon dioxide angiography.** In: Katzen BT, ed. *Radiologic Clinics of North America.* Philadelphia, Pa: Saunders; 1995;33:15–29
13. Coffey R, Quisling RG, Mickle JP, Hawkins IF Jr, Ballinger WB. **The cerebrovascular effects of intraarterial CO_2 in quantities required for diagnostic imaging.** *Radiology* 1984;51:405–409
14. Shifrin EG, Plich MB, Verstandig AG, Gomori M. **Cerebral angiography with gaseous carbon dioxide CO_2.** *J Cardiovasc Surg* 1990;31:603–606
15. Bruce W. **Anaesthetic breathing systems.** In: Scurr C, Feldman S, Soni N, eds. *Foundations of Anaesthesia.* London, England: Butterworth; 1990;673–687
16. Jöbsis F. **Noninvasive, infrared monitoring of cerebral and myocardial oxygen sufficiency and circulatory parameters.** *Science* 1977;198:1264–1267
17. Thorniley MS, Wickramasinghe YABD, Rolfe P. **Near infra-red spectroscopy: a new technique for the non-invasive monitoring of tissue and blood oxygenation in vivo.** *Biochem Soc Trans* 1988;16:978–979
18. Van Bel F, Dorrepaal CA, Benders MJNL, Zeeuwe PEM, Van de Bor M, Berger HM. **Changes in cerebral hemodynamics and oxygenation in the first 24 hours after birth asphyxia.** *Pediatrics* 1993;92:365–372
19. Pryds O, Greisen G, Skov LL, Friis-Hansen B. **Carbon dioxide-related changes in cerebral blood volume and cerebral blood flow in mechanically ventilated preterm neonates: comparison of near infrared spectroscopy and ^{133}xenon clearance.** *Pediatr Res* 1990;27:445–449
20. Brazy JE, Lewis DV, Mitnick MH, Jobsis F. **Nonivasive monitoring of cerebral oxygenation in preterm infants: preliminary observations.** *Pediatrics* 1985;75:217–225
21. Wiernsperger N, Sylvia AL, Jöbsis FF. **Incomplete transient ischemia: a non-destructive evaluation of in vivo cerebral metabolism and hemodynamics in rat brain.** *Stroke* 1981;12:864–868
22. Stauffer HM, Durunt TM, Oppenheimer MJ. **Gas embolism: roentgenologic considerations including the experimental use of carbon dioxide as an intracardiac contrast material.** *Radiology* 1956;66:686–692
23. Bettmann MA, D'Agostino R, Juravski LU, Jeffery RF, Tottle A, Goudey CP. **Carbon dioxide as an angiographic contrast agent: a prospective randomized trial.** *Invest Radiol* 1994;29 (Suppl 2):S45–S49.
24. Hawkins IF. **Carbon dioxide digital subtraction arteriography.** *AJR Am J Roentgenol* 1982;139:19–24
25. Häggendal E, Löfgren J, Nilsson NJ, et al. **Prolonged cerebral hyperemia after periods of increased cerebrospinal fluid pressure in dogs.** *Acta Physiol Scand* 1970;79:272–279
26. Lassen NA. **The luxury-perfusion syndrome and its possible reaction to acute metabolic acidosis localised within the brain.** *Lancet* 1966;2:1113–1115
27. Gourley JK, Heistad DD. **Characteristics of reactive hyperemia in the cerebral circulation.** *Am J Physiol* 1984;246:H52–H58
28. Berne RM, Rubio R, Curnish RR. **Release of adenosine from ischemic brain: effect of cerebral vascular resistance and incorporation into cerebral adenine nucleotides.** *Circ Res* 1974;35:262–271
29. Kontos HA. **Oxygen radicals in cerebral vascular injury.** *Circ Res* 1985;57:508–516
30. Smith AL, Neufeld GR, Ominsky AJ, Wollman H. **Effect of arterial CO_2 tension on cerebral blood volume, mean transit time, and vascular volume.** *J Appl Physiol* 1971;31:701–707
31. Takashima S, Ando Y. **Reflectance spectrophotometry, cerebral blood flow and congestion in young rabbit brain.** *Brain Dev* 1988;10:20–23
32. Safar P. **Resuscitation from clinical death: pathophysiologic limits and therapeutic potentials.** *Crit Care Med* 1988;16:923–941
33. Siesjö BK. **Mechanisms of ischemic brain damage.** *Crit Care Med* 1988;16:954–963
34. Thorniley MS, Wickramasinghe YABD, Rolfe P. **Near infra-red spectroscopy: monitoring cerebral tissue oxygenation non-destructively in the rat and rabbit brain.** *Biochem Soc Trans* 1988;16:980–981
35. De La Torre, Meredith J, Netsky M. **Cerebral air embolism in the dog.** *Arch Neurol* 1962;6:307–316
36. Hekmatpanah J. **Cerebral microvascular alterations in arterial air embolism.** *Adv Neurol* 1978;20:245–253
37. Klatzo I. **Disturbances of blood brain barrier in cerebrovascular disorders.** *Acta Neuropathol (Berl)* 1983;8 (Suppl):81–88
38. Klatzo I. **Pathophysiological aspects of brain edema.** *Acta Neuropathol (Berl)* 1987;72:236–239
39. Pappius HM. **Cerebral edema and the blood brain barrier.** In: Neuwelt EA, ed. *Implications of the Blood Brain Barrier and Its Manipulations.* New York, NY: Plenum: 1989;2:293–309
40. Joo F. **A unifying concept on the pathogenesis of brain oedemas.** *Neuropathol Appl Neurobiol* 1987;13:161–176
41. Joo F. **New aspects to the function of the cerebral endothelium.** *Nature* 1986;321:197–198
42. Greenwood J. **Mechanisms of blood-brain barrier breakdown.** *Neuroradiology* 1991;33:95–100
43. MacFarlane R, Moskowitz MA, Sakas DE, Tasdemiroglou E, Wei EP, Kontos HA. **The role of neuroeffector mechanisms in cerebral hyperperfusion syndromes.** *J Neurosurg* 1991;75:845–855
44. Hossman KA, Tagaki S. **Osmolarity of brain in cerebral ischemia.** *Exp Neurol* 1976;51:124–131
45. Persson LI, Johansson BB, Hansson HA. **Ultrastructural studies on blood-brain barrier dysfunction after cerebral air embolism in the rat.** *Acta Neuropathol (Berl)* 1978;44:53–56